ISSN 0036-0236, Russian Journal of Inorganic Chemistry, 2020, Vol. 65, No. 10, pp. 1541–1546. © Pleiades Publishing, Ltd., 2020.
Russian Text © The Author(s), 2020, published in Zhurnal Neorganicheskoi Khimii, 2020, Vol. 65, No. 10, pp. 1338–1344.

SYNTHESIS AND PROPERTIES OF INORGANIC COMPOUNDS

Synthesis of $CaCu_3Ti_4O_{12}$, Study of Physicochemical and Photocatalytic Properties

K. V. Ivanov[a, *], **O. V. Alekseeva**[a], **and A. V. Agafonov**[a]
[a] *Krestov Institute of Solution Chemistry, Russian Academy of Sciences, Ivanovo, 153045 Russia*
**e-mail: ivk@isc-ras.ru*

Received May 7, 2020; revised May 25, 2020; accepted May 27, 2020

Abstract—Precursor $CaCu_3Ti_4O_{12}$ has been obtained using solution method in acetic acid medium, it was annealed at 100, 200, 400, 600 800, and 1100°C. Sintered powders have been studied by physicochemical methods of analysis. According to X-ray powder diffraction, completely formed crystal structure $CaCu_3Ti_4O_{12}$ exists at 1100°C, the particle size of the prepared powder is 1–10 μm. Thermal analysis with allowance for mass spectrometric analysis system of vapor phase has revealed process mechanisms. Effect of dried at 100°C powder of precursor and $CaCu_3Ti_4O_{12}$ on the photocatalytic activity of Rhodamine B decoloration has been shown. Pseudo-first and pseudo-second order kinetics for Rhodamine B adsorption on samples annealed at 100 and 1100°C has been revealed.

Keywords: thermal treatment, synthesis, kinetics, photocatalytic activity

DOI: 10.1134/S0036023620100095

INTRODUCTION

In recent time, a large attention is attracted to the studies of photocatalytic activity of materials with perovskite structure to design photocatalysts [1, 2] useful in decontamination systems of aqueous and air media from organic molecules (dyes, pharmaceuticals) and bacteria [3–5]. The development of photocatalysts active on exposure to visible light is of special interest. However, widely known titanium dioxide used as photoactive material has drawbacks due to its low photosensitivity in visible spectral region because of large band gap width. One of the methods to extend TiO_2 absorption region to visible spectrum is the doping of titanium dioxide with transition metals or other compounds. A number of works were devoted to study metal oxides [6], hybrid [7], hetero structurized [8], and other systems.

Literature provides the data on the investigation of materials with perovskite structure such as $BaTiO_3$ [9], $SrTiO_3$ [10], $CaTiO_3$ [11], $LaFeO_3$ [12], etc., showing good photocatalytic activity. However, they have wide band gaps (>3 eV) and can be activated only in ultraviolet light [13]. The authors [14] found that $CaCu_3Ti_4O_{12}$ (**CCTO**) has two band gaps: 1.93 and 2.21 eV. Therefore the study of photocatalytic properties of CCTO, which is double cubic perovskite [15] prepared by different methods, seems to be topical because it combines the photocatalytic properties of TiO_2 [16] showing high activity in ultraviolet and CuO that absorbs visible light. The combination of properties of these oxides in CCTO should favor to photocatalytic activity in visible light resulting from charge transfer in visible light from the main to the excited state.

Titanium dioxide is known to show antimicrobial and antimycotic properties preferably on exposure to light [17]. The doping of TiO_2 with metal ions or designing nanosized composites using different oxides (CuO, Ag_2O, etc.) leads to emergence of antimicrobial activity in the dark [18–20]. The use of such materials as $CaCu_3Ti_4O_{12}$ allows one to design coatings on textile materials for medicinal purposes and aids for respiratory tract protection.

It should be noted that literature includes mainly reports on the studies of dielectric permittivity of CCTO due to its possible application in microelectronics [21, 22].

The aim of this work is to synthesize and study the structure and photocatalytic activity of CCTO.

EXPERIMENTAL

The precursor of ceramic powder of CCTO was synthesized by liquid-phase method in acetic acid medium. Initial reagents used were $Ca(OH)_2$, $Cu(CH_3COO)_2 \cdot H_2O$, $Ti(C_4H_9O)_4$ (in stoichiometric ratio CaO : CuO : TiO_2 = 1 : 3 : 4), and glacial acetic acid (all chemicals from SIGMA-Aldrich). Synthesis procedure consisted in the preparation of aqueous solution of $Cu(CH_3COO)_2 \cdot H_2O$ and a solution of calcium acetate by the reaction of $Ca(OH)_2$ with CH_3COOH (glacial). The obtained solutions were

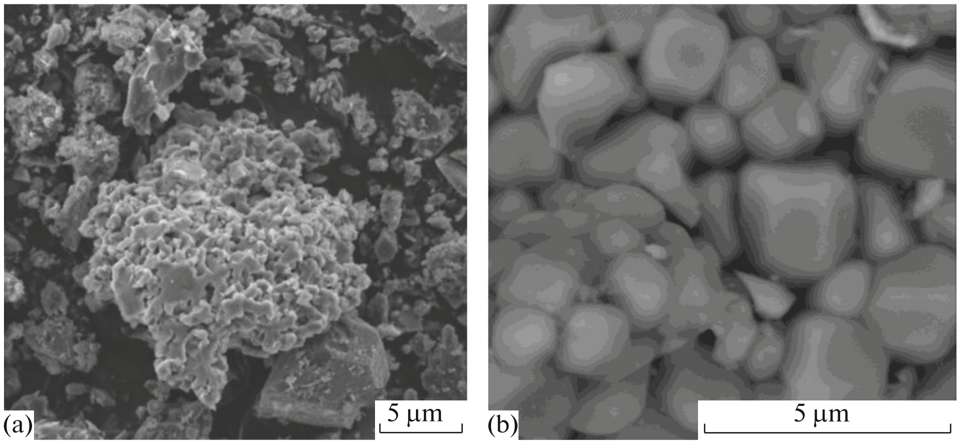

Fig. 1. SEM images of powder at (a) 100 and (b) 1100°C.

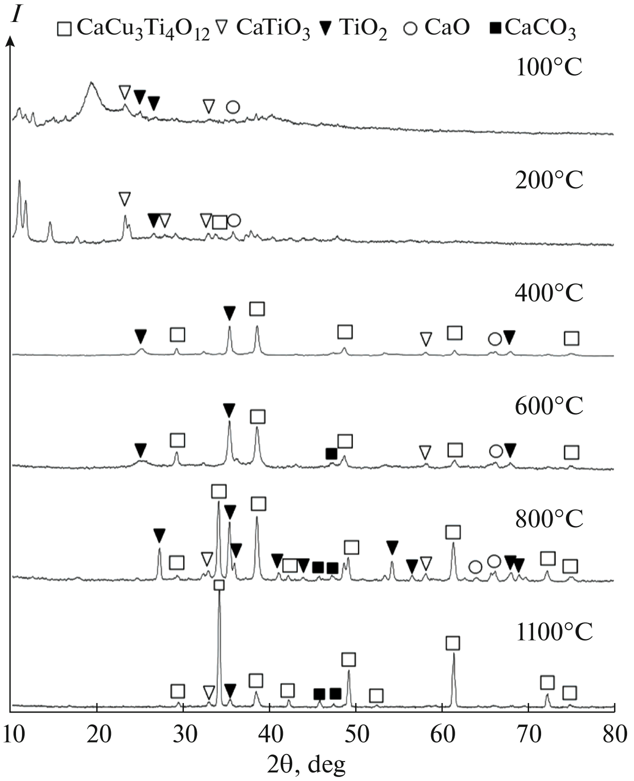

Fig. 2. XRD of prepared thermally treated powder.

mixed and stirred for 1 h at 85°C. Titanium butoxide was added dropwise to the homogeneous solution and kept for 1 h at continuous heating (85°C) and stirring. The solution was dried in a drying cabinet at 100°C until constant weight and annealed in air at temperatures 200, 400, 600, 800, and 1100°C.

The samples of thermally treated powders were studied by physicochemical methods of analysis. Powder morphology was studied by scanning electron microscopy (a Vega3 SBH Tescan microscope). Thermal analysis of the prepared powder was carried out on a Netzsch STA 409 C/CD instrument. X-ray diffraction study of the prepared powders was performed on a DRON-3M diffractometer (CuK_α radiation, voltage 40 kV). IR spectra of powders of the prepared compounds as KBr pellets were recorded on a Vertex 80v Fourier transform IR spectrometer. The photocatalytic activity of the powder was studied by spectrophotometry on exposure of rhodamine solution in a suspension of 0.043 g of photocatalyst powder in a 1-L quartz thermostated cell to ultraviolet light. A 250-W high-pressure mercury lamp with radiation maximum at 365 nm was used as a source of ultraviolet radiation. The installation was described in detail in the work [23].

RESULTS AND DISCUSSION

Physicochemical Characteristics of Prepared Materials

Figures 1a and 1b show electronic micrographs of surfaces of the obtained powders and annealed for 1 h at 100 and 1100°C. The micrographs show that the materials have polydisperse structure. Thermally treated sample at 100°C and applied voltage 5.0 kV during measurement is a combination of agglomerates as a disordered and lamellar structure. The size of these grains is 500 nm–8 μm. The sintering at 1100°C and applied voltage of 15.0 kV during recording leads to emergence of larger aggregates having a rounded cubic shape and size from 1 to 10 μm, which is caused by sintering processes and crystalline structure formation. The surface of the obtained material is a large structure with small number of pores.

The X-ray powder diffraction study of change in the crystal structure of the prepared powder during thermal treatment (Fig. 2) allowed us to reveal the process of CCTO phase formation in the range from 100 and 1100°C.

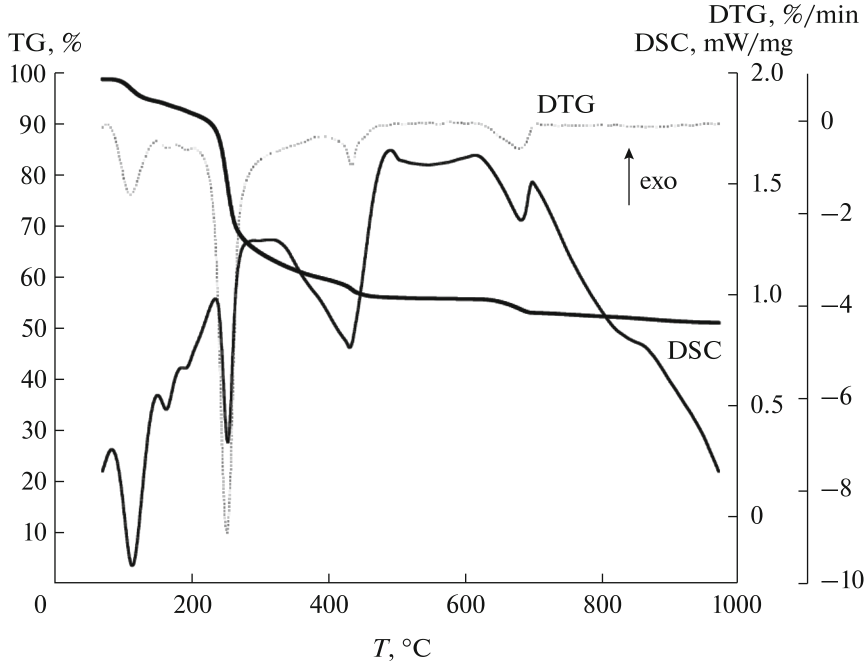

Fig. 3. Thermogram of the prepared powder.

The nucleation of $CaCu_3Ti_4O_{12}$ crystallites is observed at 400°C, which is evidenced by the presence of reflections $2\theta = 29.57°$, $38.47°$, $49.38°$, and $61.45°$. Further increase in treatment temperature is accompanied by the emergence of new reflections on diffractogram and the growth of crystalline phase of CCTO whose formation completed at 1100°C ($2\theta = 29.57°$, $34.45°$, $38.47°$, $42.36°$, $49.38°$, $52.53°$ $61.45°$, $72.32°$, $74.92°$). As Fig. 2 shows, the powders contain admixtures of calcium carbonate ($2\theta = 47.53°$, $48.52°$), titanium dioxide as rutile phase (2θ = $27.46°$, $34.88°$, $36.12°$, $41,28°$, $44,08°$, $54.37°$, $56.68°$, $68.82°$, $69.07°$), calcium oxide ($2\theta = 64.71°$, $67.97°$), and calcium titanate ($2\theta = 33.4°$, $59.68°$). Their considerable amount was found for powder annealed at 800°C. The size of crystallites calculated by the Scherrer equation ($D = 0.94\lambda/(B \cos\theta)$), at 800°C equals to 31 nm, that at 1100°C is 35 nm.

Thermal analysis of the prepared powder (Fig. 3) performed in combination with mass spectra identification for gas phase by ion current (Fig. 4) enables us to consider in detail thermal processes in the material on thermal destruction. Thermogram shows three stages. The first stage is sample heating to ~320°C, resulting in weight loss 36.5% due to removal of water, acetate groups, and acetone according to the data of mass spectra of ion currents. The formation of acetone detected in Fig. 4 seems to be caused by the decomposition of acetic acid excess on heating:

$$CH_3COOH \rightarrow (CH_3)_2CO + CO_2 + H_2O,$$

as well as acetates in the prepared powder.

The portion of gravimetric curve from 320 to 600°C (the second stage) displays weight loss (7.4%) due to decomposition of complexes of titanium isobutoxide with acetic acid to titanium dioxide and products of organic compound destruction. The subsequent change of sample weight at 600–1000°C (the third stage) corresponds to the decomposition of calcium carbonate present in material as intermediate product and formation of $CaCu_3Ti_4O_{12}$. The total weight loss of sample is 48.5%.

The IR spectra of prepared powder (Fig. 5) in temperature range 100–800°C shows absorption bands of adsorbed water in the range 3670–3250 cm^{-1}.

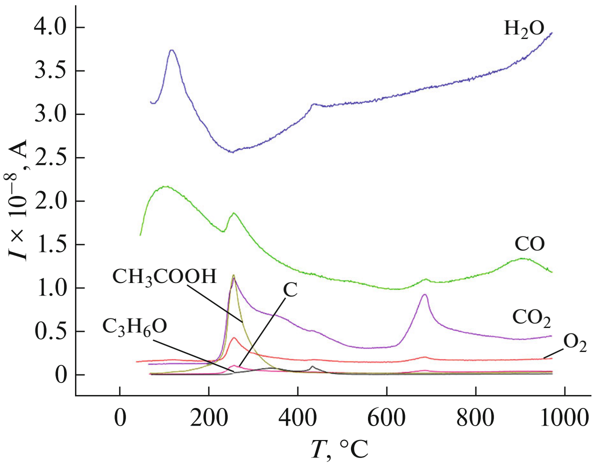

Fig. 4. Ion currents for the prepared powder.

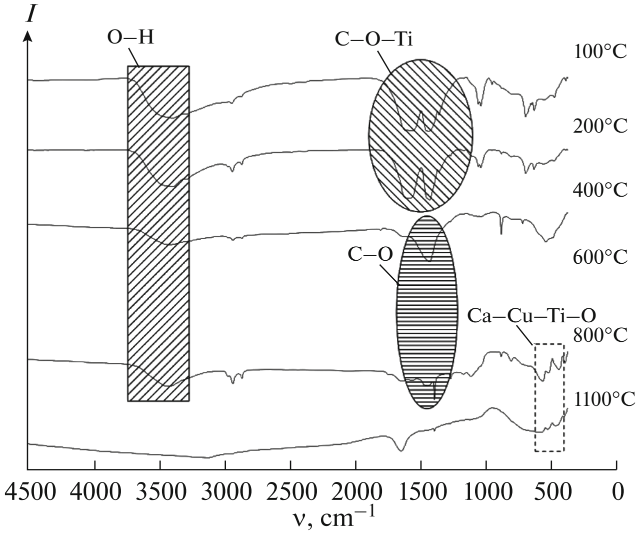

Fig. 5. IR spectra of the annealed powder.

The heating of the powder from 100 to 200°C leads to emergence of bands at 1580 and 1430 cm^{-1} corresponding to bidentate acetate bridging group. It degrades on further heating. The formation of carbonate groups corresponding to C–O vibrations at 1456 and 860 cm^{-1} seems to proceed on further heating, which is confirmed by X-ray powder diffraction and thermogravimetric analysis with allowance for evolved gases.

The IR spectrum of powder annealed at 800 and 1100°C displays bands at 561, 516, and 441 cm^{-1} indicating the presence of CCTO. The authors [24] believe that these vibrations are related to titanium ions (Ti–O 653–550 cm^{-1} and Ti–O–Ti 495–436 cm^{-1}).

Photocatalytic Measurements

The photocatalytic activity of the powder, CCTO precursor dried at 100°C and $CaCu_3Ti_4O_{12}$ powder obtained by thermal annealing at 1100°C was studied using the reaction of photocatalytic decoloration of Rhodamine B dye as an example.

Figure 6 shows change in the absorption spectra of aqueous solution of Rhodamine B on exposure to ultraviolet radiation from a 250-W high-pressure lamp with maximum at 365 nm. Absorption maximum for Rhodamine B is 552 nm. Figure 6 shows that maximum intensity decreases when irradiation time increases, solution color changes from bright violet to colorless. Adsorption spectra exhibit a shift of absorption maximum (especially in Fig. 6a) probably due to effect of the powder containing organic groups, in particular acetate, which affect the wavelength shift during irradiation of aqueous suspension and owing to solution decoloration (Fig. 6b).

The results of efficiency of photocatalytic decomposition of Rhodamine B in Fig. 7 display that the most complete degradation of the dye in aqueous solution occurs when CCTO powder obtained by the thermal treatment of precursor at 1100°C is used as a photocatalyst. In this case, dye decoloration was 84.4%, whereas the use of the powder annealed at 100°C led to decoloration of 52.1%. The difference in the values of photocatalytic activity of the powders seems to be due to the difference in the phase composition, crystallinity degree, and the presence of active centers.

To analyze the process of dye adsorption, we used a general kinetic model of chemical reactions, namely the Lagergren model of pseudo-first and pseudo-second order kinetics. The pseudo-first-order rate model

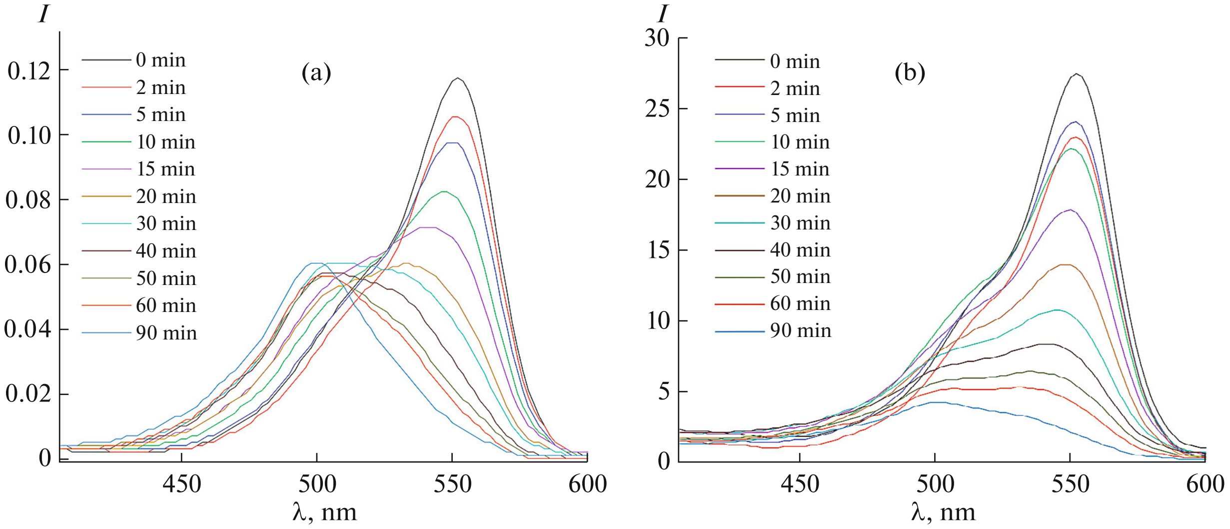

Fig. 6. Absorption spectra of Rhodamine B on exposure to ultraviolet in aqueous solution by the powder annealed at (a) 100, (b) 1100°C.

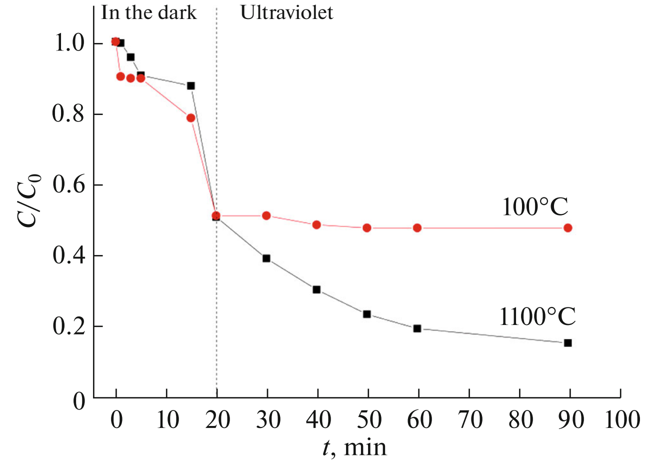

Fig. 7. Photocatalytic decomposition of Rhodamine B on catalyst powders annealed at 100 and 1100°C in the dark and on exposure to ultraviolet.

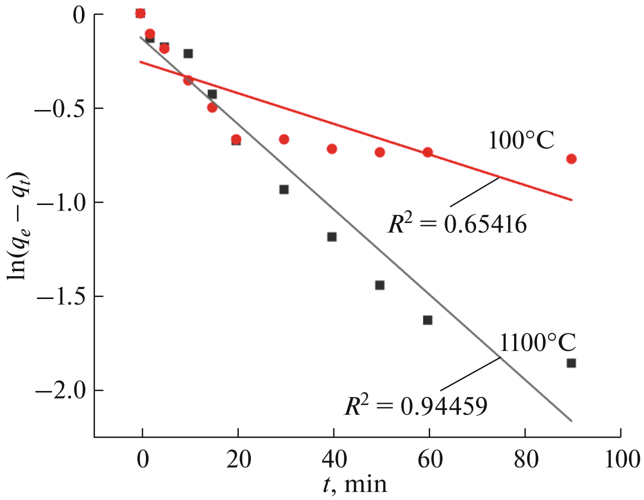

Fig. 8. Pseudo-first-order model kinetics for Rhodamine B adsorption on samples annealed at 100 and 1100°C.

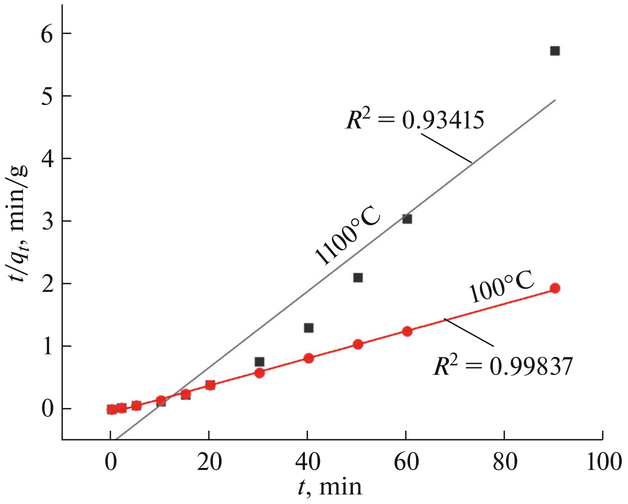

Fig. 9. Pseudo-second-order model kinetics for Rhodamine B adsorption on samples annealed at 100 and 1100°C.

suggested by Lagergren [25] is expressed by the equation:

$$\ln(q_e - q_t) = \ln q_e - k_1 t,$$

where q_e and q_t (mg/g) is the amount of adsorbed Rhodamine B in equilibrium state and at the definite time point, respectively; t is the time of contact (min); k_1 is pseudo-first-order rate constant (min^{-1}) determined from the slope of section $\ln(q_e - q_t)$ to t.

The linearized pseudo-second-order model is expressed by the following equation [26]:

$$\frac{t}{q_t} = \frac{1}{k_2 q_e^2} + \frac{t}{q_e},$$

were k_2 is the pseudo-second-order rate constant, g/(mg min).

According to the plot shown in Fig. 8 for the model of pseudo-first-order kinetics, the values of R^2 (correlation coefficient) of Rhodamine B adsorption on samples are within 0.65 to 0.94. Experimentally observed kinetics for adsorption on powder dried at 100°C is insufficiently described by the pseudo-first-order model because of linear dependences only at short time of phase contact. The obtained shape of dependence in the noted coordinates probably indicates the mixed diffusion kinetics of sorption process and provides no possibility to unambiguously reveal limiting stage. Rate constants for pseudo-first-order kinetic model were 0.00814 min^{-1} for powder CCTO precursor dried at 100°C and 0.02261 min^{-1} for $CaCu_3Ti_4O_{12}$.

The pseudo-second-order kinetics of Rhodamine B adsorption model (Fig. 9) provides the R^2 value of 0.99837 for the sample annealed at 100°C and 0.93415 for the sample annealed at 1100°C, the rate constant is 0.02 and 0.06, respectively. In summary, pseudo-first-order model describes the kinetics for CCTO obtained by thermal treatment at 1100°C rather well. The pseudo-second-order model agree well with the sample dried at 100°C, which indicates that adsorption includes both chemical and physical sorption [26].

CONCLUSIONS

Compound $CaCu_3Ti_4O_{12}$ was obtained by the thermal treatment at 1100°C of precursor prepared by solution method. Scanning electron microscopy showed that the size of particles of the synthesized powder dried at 100°C is 1–2 μm, while that of CCTO is 2–5 μm. The processes occurred on the thermal treatment of the prepared matter were studied by a number of physicochemical methods of analysis. It was revealed that the formation of $CaCu_3Ti_4O_{12}$ phase completes at 1100°C. Adsorption kinetics for powder with $CaCu_3Ti_4O_{12}$ crystalline phase corresponds to pseudo-first-order model, while that for precursor agrees with pseudo-second-order model. It was found that, over the first 15 min, more than 30% of Rhodamine B is removed under the action the obtained samples in the dark. The highest photocatalytic activity is shown by the powder with CCTO crystalline phase where Rhodamine B removal is ~84.4%.

ACKNOWLEDGMENTS

The authors thank to the Shared Facility Center, Upper Volga Regional Center for Physicochemical Studies.

FUNDING

This work was supported by the Ministry of Science and Higher Education of the Russian Federation (State assignment no. 01201260483) and partially supported by the Russian Foundation for Basic Research (project no. 18-43-370015).

CONFLICT OF INTEREST

The authors declare no conflict of interest.

REFERENCES

1. A. M. Huerta-Flores, D. Sánchez-Martínez, M. R. Hernández-Romero, et al., J. Photochem. Photobiol., A **368**, 70 (2019). https://doi.org/10.1016/j.jphotochem.2018.09.025
2. Y. Hu, L. Mao, X. Guan, et al., Renewable and Sustainable Energy Rev. **119**, 109527 (2020). https://doi.org/10.1016/j.rser.2019.109527
3. J. Ahmad and K. Majid, New J. Chem. **42**, 3246 (2018). https://doi.org/10.1039/C7NJ03617E
4. E. K. Papynov, O. O. Shichalin, I. Yu. Buravlev, et al., Russ. J. Inorg. Chem. **65**, 263 (2020). https://doi.org/10.1134/S0036023620020138
5. O. G. Ellert, S. A. Nikolaev, D. A. Maslov, et al., Russ. J. Inorg. Chem. **63**, 1403 (2018). https://doi.org/10.1134/S0036023618110049
6. W. Wan, R. Zhang, M. Ma, et al., J. Mater. Chem. A **6**, 754 (2018). https://doi.org/10.1039/C7TA09227J
7. X. Yang, Z. Wen, Z. Wu, et al., Inorg. Chem. Front. **5**, 687 (2018). https://doi.org/10.1039/C7QI00752C
8. Z. Su, H. Li, P. Chen, et al., Catal. Sci. Technol. **7**, 5105 (2017). https://doi.org/10.1039/C7CY01207A
9. J. Li, G. Zhang, S. Han, et al., Chem. Commun. **54**, 723 (2018). https://doi.org/10.1039/C7CC07636C
10. Z. Wu, Y. Zhang, X. Wang, et al., J. Clim. **41**, 5678 (2017). https://doi.org/10.1039/C7NJ00522A
11. K. V. Ivanov, A. V. Agafonov, and O. V. Alekseeva, Izv. Vyssh. Uchebn. Zaved., Khim. Khim. Tekhnol. **59** (6), 83 (2016). https://doi.org/10.6060/tcct.20165906.5384k
12. K. Xu and J. Feng, RSC Adv. **7**, 45369 (2017). https://doi.org/10.1039/C7RA08715B
13. G. Zhang, G. Liu, and L. Wang, Chem. Soc. Rev. **45**, 5951 (2016). https://doi.org/10.1039/C5CS00769K
14. J. H. Clark, M. S. Dyer, R. G. Palgrave, et al., J. Am. Chem. Soc. **133**, 1016 (2011). https://doi.org/10.1021/ja1090832
15. N. A. Madhar and B. Ilahi, et al., Sci. Reports **6**, 18557 (2016). https://doi.org/10.1038/srep18557
16. L. N. Ribeiro, A. C. S. Fonseca, E. F. M. Silva, et al., Chem. Eng. Process: Process Intensification **147**, 107792 (2020). https://doi.org/10.1016/j.cep.2019.107792
17. J. Li, Z. Wu, M. Su, et al., J. Vacuum **176**, 109346 (2020). https://doi.org/10.1016/j.vacuum.2020.109346
18. X. He, G. Zhang, X. Wang, et al., Ceram. Int. **43**, 16185 (2017). https://doi.org/10.1016/j.ceramint.2017.08.196
19. Y. Jin, Z. Dai, F. Liu, et al., Water Res. **47**, 1837 (2013). https://doi.org/10.1016/j.watres.2013.01.003
20. S. Chen, Y. Guo, H. Zhong, et al., Chem. Eng. J. **256**, 238 (2014). https://doi.org/10.1016/j.cej.2014.07.006
21. P. Liu, Y. Lai, Y. Zeng, et al., J. Alloys Compd. **650**, 59 (2015). https://doi.org/10.1016/j.jallcom.2015.07.247
22. C. C. Homes, T. Vogt, S. M. Shapiro, et al., Science **293**, 673 (2001). https://doi.org/10.1126/science.1061655
23. T. V. Gerasimova, O. L. Evdokimova (Galkina), A. S. Kraev, et al., Microporous Mesoporous Mater. **235**, 185 (2016). https://doi.org/10.1016/j.micromeso.2016.08.015
24. L. C. Kretly, A. F. L. Almeida, P. B. A. Fechine, et al., J. Mater. Sci, Mater. Electron. **15**, 657 (2004).
25. S. Lagergren, Kung Sven Veten Hand **24**, 39 (1898). https://doi.org/10.1023/B:JMSE.0000038920.30408.77
26. Y. S. Ho and G. McKay, Process Biochem. **34**, 451 (1999). https://doi.org/10.1016/s0032-9592(98)00112-5

Translated by I. Kudryavtsev